Biochemical and genetic characterization of a novel enzyme of pentitol metabolism: D-arabitol-phosphate dehydrogenase

Mira POVELAINEN*, Elena V. ENEYSKAYA†, Anna A. KULMINSKAYA†, Dina R. IVANEN†, Nisse KALKKINEN‡, Kirill N. NEUSTROEV† and Andrei N. MIASNIKOV*[1]

*Danisco Cultor Innovation, Sokeritehtaantie 20, Kantvik 02460, Finland, †Petersburg Nuclear Physics Institute, Gatchina, Leningrad District 188300, Russia, and ‡Institute of Biotechnology, University of Helsinki, Viikinkaari 9, Helsinki 00014, Finland

An enzyme with a specificity that has not been described previously, D-arabitol-phosphate dehydrogenase (APDH), has been purified from cell lysate of *Enterococcus avium*. SDS/PAGE indicated that the enzyme had a molecular mass of 41 ± 2 kDa, whereas a molecular mass of 160 ± 5 kDa was observed under non-denaturing conditions, implying that the APDH may exist as a tetramer with identical subunits. Purified APDH was found to have a narrow substrate specificity, converting only D-arabitol 1-phosphate and D-arabitol 5-phosphate into xylulose 5-phosphate and ribulose 5-phosphate, respectively, in the oxidative reaction. Both NAD^+ and $NADP^+$ were accepted as cofactors. Based on the partial protein sequences, the APDH gene was cloned. Homology comparisons place APDH within the medium-range dehydrogenase family. Unlike most members of this family, APDH requires Mn^{2+} but no Zn^{2+} for enzymic activity. The DNA sequence surrounding the gene suggests that it belongs to an operon that also contains several components of phosphotransferase system. Both biochemical evidence and protein sequence homology comparisons indicate that similar enzymes are widespread among the Gram-positive bacteria. Their apparent biological role is to participate in arabitol catabolism via the 'arabitol phosphate route', similar to the ribitol and xylitol catabolic routes described previously.

Key words: *Enterococcus avium*, NADH-dependent dehydrogenase, pentitol phosphate metabolism, xylulose 5-phosphate.

INTRODUCTION

The best-characterized catabolic pathways of polyols start with the uptake of a neutral polyol by the cell followed by its oxidation to the corresponding keto-sugar catalysed by an intracellular polyol-dehydrogenase. The keto-sugars are subsequently phosphorylated to form the intermediates of the glycolytic or pentose phosphate pathways. Alternative pathways, where the polyol is taken up and phosphorylated [typically by a phosphotransferase system (PTS)], followed by oxidation of the resulting polyol phosphates by polyol-phosphate dehydrogenases, are also rather common in bacteria. Particularly, metabolic routes involving hexitol phosphates have been the subject of many studies [1–4]. Pentitols can also be catabolized via pentitol phosphate intermediates [5]; however, studies of such pathways have been limited to a few species of *Lactobacillus* and two pentitols: ribitol and xylitol [6]. Understanding the enzymology of pentitol phosphate metabolism has considerable practical importance, since these compounds are believed to play a central role in the cariostatic activity of pentitol sweeteners [7]. Two types of dehydrogenases involved in arabitol assimilation via pentulose intermediates (Scheme 1) have been characterized [8–10], but the evidence for arabitol assimilation via the pentitol phosphate pathway has been controversial. Hausman and London [6] concluded that in *Lactobacillus casei* D-xylitol-phosphate dehydrogenase can also oxidize D-arabitol 5-phosphate (Arb5P) and is probably involved in arabitol assimilation by such strains. This hypothesis implies that the reduction of D-xylulose 5-phosphate (Xlu5P) and D-ribulose 5-phosphate (Rlu5P) catalysed by this enzyme leads to products with different stereochemical configurations around C-2. Such specificity would be very unusual for an NAD^+-dependent dehydrogenase. In this study we demonstrate that a dehydrogenase with specificity towards D-arabitol phosphate can be isolated from a pentitol-utilizing *Enterococcus avium* strain as well as several other Gram-positive bacteria. We also present initial structural and functional characterization of this novel enzyme.

MATERIALS AND METHODS

Materials

Polyols and polyol phosphates were purchased from Sigma (St. Louis, MO, U.S.A.). Xylitol 5-phosphate was synthesized according to previously described methods [11]. D-Arabitol 1-phosphate (Arb1P) and Arb5P were synthesized by $NaBH_4$ reduction of Xlu5P and arabinose 5-phosphate followed by chromatographic separation [12]. The purity of substrates was checked by 500 MHz ^{1}H-NMR spectroscopy. Restriction enzymes, high-fidelity DNA polymerase and T4 ligase were purchased from Roche (Zurich, Switzerland). Oligonucleotides were purchased from MedProbe (Oslo, Norway).

Bacterial strains and culture conditions

E. avium ATCC 35665 was from American Type Culture Collection (Manassas, VA, U.S.A.). This strain was cultivated at 37 °C with shaking (150 rev./min) for 36 h in a medium containing 5.6 g/l BLA (Biolog lactic acid bacteria) suspension broth (Biolog, Hayward, CA, U.S.A.), 2 g/l K_2HPO_4, 5 g/l

Abbreviations used: APDH, D-arabitol-phosphate dehydrogenase; Arb1P, D-arabitol 1-phosphate; Arb5P, D-arabitol 5-phosphate; DTT, dithiothreitol; Orf, open reading frame; PHMB, 4-hydroxymercuribenzoic acid; PTS, phosphotransferase system; Rlu5P, D-ribulose 5-phosphate; Xlu5P, D-xylulose 5-phosphate.

[1] To whom correspondence should be addressed (e-mail andrei.miasnikov@danisco.com).

The nucleotide sequence data reported will appear in the GenBank® Nucleotide Sequence Database under the accession number AY078980.

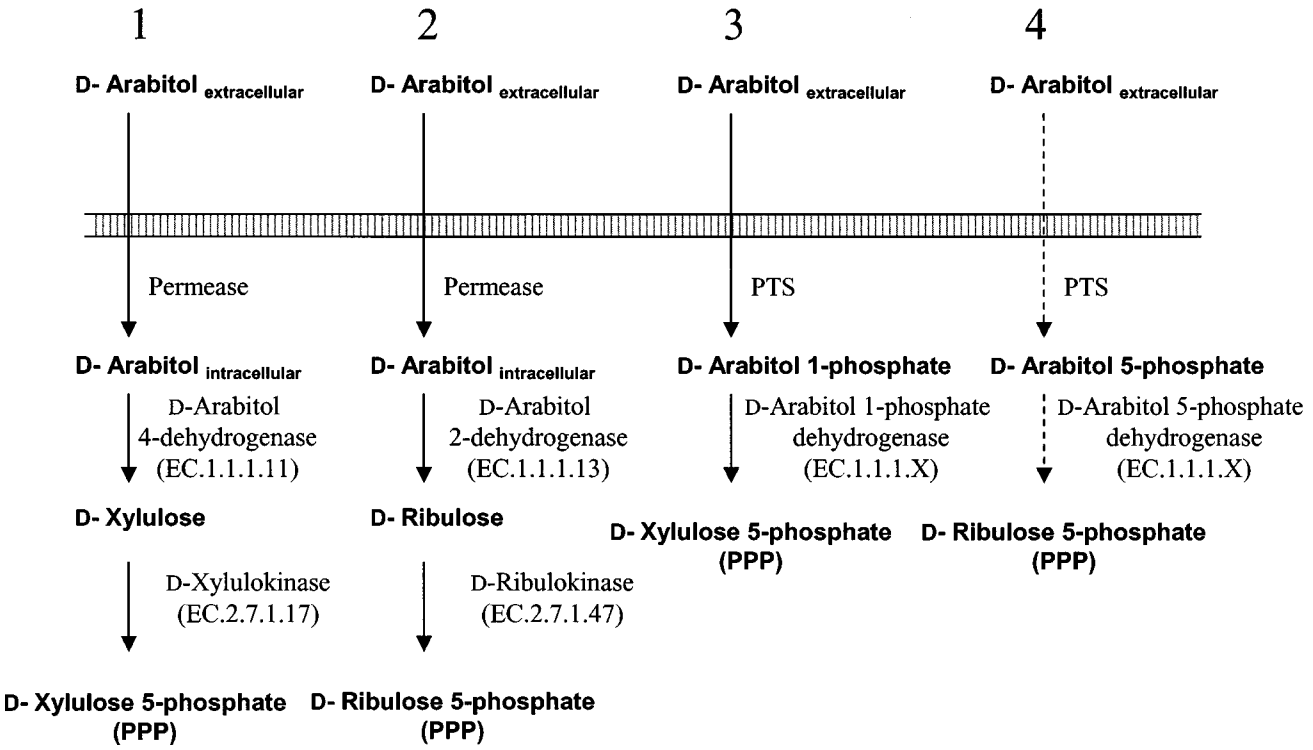

Scheme 1 Different catabolic routes for D-arabitol

Route 1 is common in bacteria and route 2 is typical in yeast. Route 3 is the most probable arabitol catabolic route in *E. avium* and several other Gram-positive bacteria. Route 4 may be operating alongside route 3 in the same strains, although evidence in favour of this route is weak. PPP, pentose phosphate pathway.

NaCl, 0.02 g/l $MgSO_4$, 0.05 g/l $MnCl_2$, 2 g/l ammonium citrate, 20 g/l xylitol and 0.16 ml of Tween 80. *Bacillus halodurans* JCM 9153 was from the Japan Collection of Microorganisms (Wako, Japan). *Bacillus subtilis* strain BD170 was obtained from the *Bacillus* Genetic Stock Centre (Ohio State University, Columbus, OH, U.S.A.).

Purification of D-arabitol-phosphate dehydrogenase (APDH)

All steps were carried out at 4 °C. Cells from 5 l of culture medium were separated by centrifugation (3000 ***g***, 20 min), washed with water and re-suspended in 20 mM Tris/HCl buffer, pH 7.2, and 3 mM dithiothreitol (DTT; buffer A). Cells were incubated with 0.3 % (w/v) lysozyme (Sigma) at 20 °C for 60 min, sonicated (3 × 20 s) and centrifuged (12000 ***g***, 20 min). The supernatant was dialysed against buffer A, applied to a DEAE 5PW column (21.5 mm × 159 mm; Amersham Biosciences, Uppsala, Sweden) equilibrated with the same buffer, and eluted with a linear gradient (0–1 M) of NaCl (total volume, 100 ml) at a flow rate of 3 ml/min. Fractions containing APDH activity were pooled, concentrated using an Amicon PM-30 membrane to 10 ml, and dialysed against 20 mM Tris/HCl buffer, pH 7.8, supplemented with 3 mM DTT. This material was further fractionated by chromatography on a MonoQ HR(5/5) column (Amersham Biosciences) with a linear gradient (0–1 M) of NaCl in the same buffer (total volume, 24 ml). The elution flow rate of 0.6 ml/min was used. The fractions with APDH activity were pooled and applied to a Sepharose Blue CL 6B column (10 mm × 5 mm; Amersham Biosciences) equilibrated with 50 mM Tris/HCl buffer, pH 8.0, 100 mM NaCl and 3 mM DTT. Fractions containing APDH activity were eluted with 3 mM NADH in the equilibration buffer (total volume, 32 ml; elution flow rate, 0.8 ml/min). Finally, the enzyme solution was loaded on to a Phenyl-Superose HR 5/5 column (Amersham Biosciences) equilibrated with 30 mM Tris/HCl, pH 7.4/1.7 M $(NH_4)_2SO_4$, and eluted with a linear gradient (0–30 mM) of Tris/HCl buffer, pH 7.4 (total volume, 40 ml; flow rate, 0.6 ml/min). Purified APDH was dialysed against 30 mM Tris/HCl buffer, pH 7.2.

General methods

Determination of the APDH molecular mass under non-denaturing conditions was performed using a Superose 12 (10 mm × 300 mm; Amersham Biosciences). The column was equilibrated with 200 mM Tris/HCl buffer, pH 7.2, containing 0.1 mM glutathione and 100 mM NaCl, and calibrated using a protein molecular-mass standards kit (MW-GF-200; Sigma) for the molecular-mass range 12000–200000 Da (elution flow rate, 0.4 ml/min). The molecular mass of the protein under denaturing conditions was estimated by SDS/PAGE on a 10 % polyacrylamide gel according to the method of Laemmli [13] using the molecular-mass calibration standards kit LMW (14400–94000 Da) from Amersham Biosciences. Native electrophoresis was performed in accordance with [9] using for calibration the molecular-mass standards kit MW-ND-500 (Sigma) covering a molecular-mass range of 14000–500000 Da. Isoelectric focusing was performed on SERVALYT® PRECOTES® plates 3-10 (Serva Electrophoresis GmbH, Heidelberg, Germany). Protein concentrations during purification were determined by the method of Lowry using BSA as a standard [14]. The concentration of pure APDH was estimated by UV absorption spectrophoto-

metry at 280 nm using a specific absoption coefficient of $0.8\,l \cdot g^{-1} \cdot cm^{-1}$. ^{1}H-NMR spectra and ^{13}C-NMR spectra were recorded with an AMX-500 Bruker spectrometer. Metal analysis was performed with Perkin Elmer model 2380 atomic absorption spectrometer with an acetylene/air flame. Reported metal content values are averages of four to six parallel measurements using at least two different batches of enzyme (or apo-enzyme in the metal reconstitution experiments). DNA was manipulated by standard procedures [15]. All PCRs were performed with a PTC-225 DNA Engine (MJ Research, Watertown, MA, U.S.A.).

Enzymic properties and kinetic analysis

The measurement of enzyme activity in the reductive reaction of Xlu5P was performed at 20 °C by following the rate of oxidation of NADH at 340 nm in 0.2 ml of a solution containing 20 mM Tris/HCl, pH 7.2, 1 mM DTT, 0.07 mM NADH, 0.2 mM Xlu5P and about 1 m-unit of enzyme. A system without sugar phosphate was used as a control. The reaction was initiated by the addition of sugar phosphate. One unit of enzyme activity was defined as an amount catalysing the oxidation of 1 μmol of NADH in 1 min under the described conditions. Enzyme activity in the oxidative direction was measured in 20 mM Tris/HCl, pH 8.5, 1 mM DTT and 0.5 mM NAD^+, Arb1P or Arb5P.

To determine the pH optimum, the APDH activity was measured in both oxidative and reductive directions under normal conditions, except that the standard assay buffer was replaced with a series of 100 mM buffer solutions supplemented with 2 mM DTT: pH 3.0–5.5, sodium acetate buffer; pH 5.5–7.0, MES buffer; pH 7.0–9.0, Tris/HCl buffer.

The effect of metal ions, anions and 4-hydroxymercuribenzoic acid (PHMB) on the enzyme activity was evaluated by incubating each of them with purified APDH (2–3 units/ml) in 20 mM Tris/HCl, pH 7.2 (buffer B), at 20 °C for 5 and 30 min followed by a 100-fold dilution and a standard activity assay. The second-order rate constant of EDTA inactivation of the enzyme was determined according to the method described in [16]. The enzyme (0.1–0.2 unit/ml or 0.05–0.1 μM tetramer) was incubated with different concentrations of EDTA (in the 0–2 mM range) at 20 °C. Aliquots of 10 μl were withdrawn at 10 min intervals for 1 h, followed by immediate 20-fold dilution into the activity assay reaction mixture (20 mM Tris/HCl, pH 7.2, 1 mM DTT, 0.07 mM NADH and 0.2 mM Xlu5P) and measurement of activity. On a preparative scale, the apo-enzyme was typically obtained by adding EDTA to 1–1.2 ml of a 20–40 units/ml (10–20 μM enzyme tetramer) solution of APDH to the final concentration of 3 mM and incubating for 30 min at room temperature. Excess EDTA and EDTA–metal complex were subsequently removed by gel filtration on a 5 mm × 200 mm column of Sephadex G-50 (fine) equilibrated with buffer B containing 0.5 mM DTT. Electron spin resonance spectroscopy with a SE/X-2544 ESR spectrometer (Radiopan, Poznan, Poland) was used to control the concentration of residual EDTA in apo-APDH according to the method described by Kayestha et al. [17]. All preparations contained less than 0.1 mM residual EDTA. Apo-APDH could be stored for about 48 h at 4 °C retaining full ability to be reconstituted with Mn^{2+}. Reconstitution of EDTA-treated APDH with different metal ions was studied by incubating the solution of apo-enzyme at 2–3 mg/ml (12.5–19 μM enzyme tetramer) in buffer B containing 0.5 mM DTT with various metal ions at concentrations in the 10–50 mM range (20 °C). This was followed by dialysis against three changes of 500-fold excess of buffer B containing 0.5 mM DTT. The metal-reconstituted enzyme preparations used in atomic adsorption analysis were dialysed once against the same buffer followed by ion-exchange chromatography on Mono Q column using stepwise elution with 300 mM NaCl. Finally, the enzyme-containing fractions were dialysed against buffer B containing 0.5 mM DTT (2 × 1 l). The chromatography and all dialyses were carried out at 4 °C.

Double-reciprocal primary plots of velocity against Xlu5P and NADH were obtained by fitting the experimental data to equations developed for a ternary-complex mechanism and reported in detail by Neuberger et al. [9]. The same procedures were applied for the oxidative reaction with Arb1P and Arb5P as a substrate and NAD^+ as a cofactor. $NADP^+$ and NADPH were tested in the same manner in the forward and reverse directions using Xlu5P and Arb1P in suitable conditions. Each kinetic constant was calculated from a set of measurements that included four or five different concentrations of a substrate and a cofactor.

Products of the oxidative and reductive reactions were analysed after the incubation of APDH (10–100 m-units) with different substrates under standard reaction conditions. The reaction mixture was then treated with a phosphatase (Sigma catalogue no. P 4252) [18] and the resulting polyols were analysed with an Aminex HPX-87P column (Bio-Rad Laboratories, Hercules, CA, U.S.A.) at 70 °C using isocratic elution with water and refractive-index detection. Alternatively, polyols were acetylated and analysed by GLC-MS [19]. Specificity of the enzyme was studied with various polyols and polyol phosphates under the conditions described above.

Sequencing of *E. avium* APDH and cloning of the APDH gene

The Coomassie Brilliant Blue-stained APDH band from SDS/PAGE was in-gel digested with trypsin and the peptides were extracted [20,21]. For possible protein identification the extracted peptides were analysed by mass mapping with a Biflex MALDI-TOF (matrix-assisted laser-desorption ionization–time-of-flight) mass spectrometer (Bruker, Franzen Analytik, Bremen, Germany). For chemical sequencing the peptides were separated by micro-reversed-phase chromatography and selected peptides subjected to Edman degradation using a Procise 494 HT sequencer [19].

PCR with degenerate primers was carried out using the following programme: five cycles of 93 °C for 45 s, 50 °C for 45 s and 72 °C for 3 min, followed by 20 cycles of 93 °C for 45 s, 60 °C for 45 s and 72 °C for 3 min. For hybridization screening, DNA probes were labelled with the DIG High Prime Labelling system (Roche) according to the instructions given by the manufacturer. Chromosomal DNA was isolated from *E. avium* and *B. halodurans* essentially by the method described in *Molecular Biological Methods for Bacillus* [22]. The *E. avium* gene library was constructed by conventional techniques in *Bam*HI-digested λZAP vector (Stratagene, La Jolla, CA, U.S.A.) using the 3–8 kb fraction of a *Sau*3A partial digest of *E. avium*. The DNA sequencing service was purchased from MedProbe. Amino acid and nucleotide sequence homology searches were performed using the BLAST service provided by the NCBI.

Construction of the expression vector

The expression vector was a derivative of pGT23, described by Kerovuo et al. [23]. *B. subtilis deg*Q36 promoter [24] modified to inactivate a presumptive catabolite-responsive element site [25] was amplified from *B. subtilis* ATCC 6051 genomic DNA using oligonuclotide primers oDEGQ 5 (5′-GGAGTCGACCATGG-GAGCACCTCGCAAAAAAGG-3′) and oDEGQM 3 (5′-GG-AGAATTCACCTCCTTTCAGAGTCCCGGGTATTTGA-TCTGTTACTAATAGTGTATCTGCTTTCGG-3′). The PCR product was digested with *Sal*I and *Eco*RI and ligated to *Sal*I/

*Eco*RI-digested pGT23 to generate pGT74. The kanamycin-resistance gene was amplified from pDG738 (*Bacillus* Genetic Stock Centre) using primers oKAN5 (5′-CGATAGTACTT-GCTTGAAACCCAGGACAAT-3′) and oKAN3 (5′-CGATG-GATCCGGGACCCCCTATCTAGCGAAC-3′). *Sca*I/*Bam*HI-digested PCR product was ligated with *Sna*BI/*Bcl*I-digested pGT74, generating pGTK74. The coding sequence of the APDH gene was amplified from *E. avium* (ATCC 35665) genomic DNA using oligonucleotide primers oXPDH 52 (5′-GGTGAATT-CATGAGTAAAACAATGAAGGGTGTTTCCAAGC-3′) and oXPDH 31 (5′-GGTGGATCCTCTAGAATTTTTGGACAG-CTTCCTTGATTC-3′). The PCR product was digested with *Eco*RI and *Bam*HI and ligated to *Eco*RI- and *Bam*HI-digested pGTK74. The resulting plasmid was designated pGTK74 (APDH3). *B. subtilis* was transformed by the 'Paris' method [26].

RESULTS AND DISCUSSION

The APDH activity was routinely determined by measuring the reduction of Xlu5P. The enzyme was purified 240-fold from crude cellular extract of *E. avium* in four chromatographic steps with a yield of 8 % of the initial activity and a specific activity of 12 units · mg^{-1}. The resulting preparation appeared homogeneous on SDS/PAGE, revealing a single polypeptide band with an estimated molecular mass of 41 ± 1 kDa. Analytical gel filtration on a Superose 12 column revealed a single symmetrical APDH peak corresponding to 160 ± 5 kDa. Essentially identical estimates were obtained using native PAGE. Taken together, all these observations led us to the conclusion that in its native state APDH is a tetramer. The isoelectric point of the APDH was 6.4. The maximal catalytic activity of APDH in the reductive reaction was found at pH 6.8–7.3 and in the oxidative reaction at pH 8.3–8.6. The same pH optima in both reductive and oxidative reactions were observed using $NADP^+$ and NADPH as cofactors.

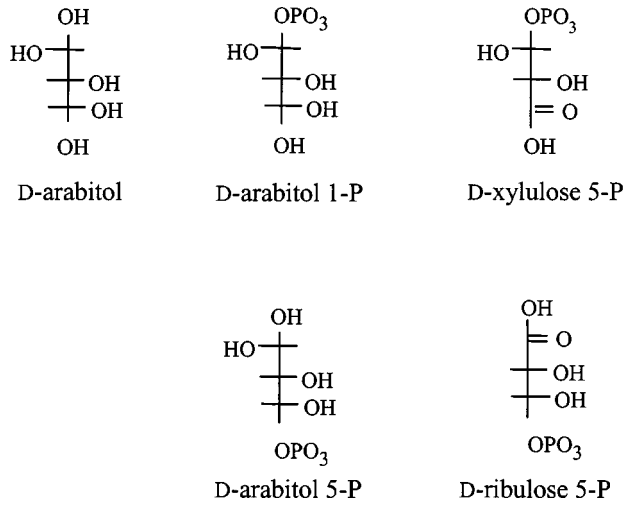

Figure 1 Structural formulae of the two arabitol phosphates and some closely related compounds

Note that the formula for Xyl5P is drawn 'upside-down' to emphasize its structural relatedness to Arb1P.

Xlu5P was incubated with the either native or recombinant APDH in the presence of NADH, followed by treatment of the reaction products with alkaline phosphatase. When the reaction products were analysed by HPLC, only arabitol and small amounts of xylulose were observed (see Figure 1 for an illustration of the structural relationships between arabitol phosphates and pentulose phosphates). A very similar product profile was obtained when the experiment was conducted using Rlu5P rather than Xlu5P as the substrate. The initial velocity of the APDH-catalysed reduction of Rlu5P was estimated at 2–3 % of the Xlu5P reduction rate. Products of the APDH-catalysed oxidation of Arb1P by NAD^+ were analysed by HPLC and GLC-MS after dephosphorylation of the reaction products. In addition to arabitol, only xylulose was detected in these analyses. Arb5P was also observed to be a substrate for APDH resulting in Rlu5P production. The initial rate of the APDH-catalysed oxidation of Arb5P was eight times lower than for Arb1P. No oxidation by APDH of xylitol 5-phosphate, D-sorbitol, D-mannitol or xylitol with NAD^+ could be detected. Likewise, erythrose 4-phosphate and ribose 5-phosphate were not reduced by APDH.

Thus substrate specificity of APDH from *E. avium* seems to be limited to oxidation of Arb1P to Xlu5P and Arb5P to Rlu5P using either NAD^+ or $NADP^+$ as cofactors. Therefore, the name 'APDH', without specification of the position of the oxidized hydroxyl group, seems to be the best working name for this enzyme.

Table 1 summarizes kinetic parameters obtained for the oxidative and reductive reactions of APDH catalysis. Figure 2 shows primary plots for the activity of the enzyme towards Xlu5P and NADH. These plots clearly indicate that APDH kinetics are consistent with a ternary-complex mechanism. As can be seen from Table 1, the value for $K_m^{Xlu5P,NADH}$ of 0.083 mM is three orders of magnitude lower than the value for Arb1P (10.65 mM), while the V_{max} of the Xlu5P reduction reaction is about 12-fold higher than that for the oxidative reaction. Kinetic parameters of the oxidative and reductive reactions using $NADP^+$ and NADPH as cofactors are also listed in Table 1. The rates of both reductive and oxidative reactions with NAD^+ and NADH as cofactors were about 14 times higher than with $NADP^+$ and NADPH.

The metal content of APDH purified from *E. avium* was analysed by atomic absorption spectrometry. Pure APDH contains 4.05 ± 0.02 ions of Mn^{2+} and less than 0.1 mol of Zn^{2+}, Mg^{2+}, Ca^{2+} and other bivalent ions (Cu^{2+}, Cd^{2+}, Co^{2+} and Fe^{2+})

Table 1 Kinetic data obtained for the purified APDH from *E. avium*

Polyol substrate and reaction direction	Substrate K_m (mM)		Co-factor K_m (mM)		Ternary-complex K_m (mM^2)		V_{max} (μmol/min per mg)	
Xlu5P, reductive	K_m^{Xlu5P}	0.23 ± 0.01	K_m^{NADH}	0.021 ± 0.001	$K_m^{Xlu5P,\ NADH}$	0.083 ± 0.004	$V_{max}^{Xlu5P,\ NADH}$	14.0 ± 0.2
Arb1P, oxidative	K_m^{Arb1P}	2.9 ± 0.1	$K_m^{NAD^+}$	0.80 ± 0.04	$K_m^{Arb1P,\ NAD^+}$	10.7 ± 0.5	$V_{max}^{Arb1P,\ NAD^+}$	1.2 ± 0.02
Arb5P, oxidative	K_m^{Arb5P}	0.63 ± 0.03	$K_m^{NAD^+}$	0.71 ± 0.03	$K_m^{Arb5P,\ NAD^+}$	0.72 ± 0.04	$V_{max}^{Arb5P,\ NAD^+}$	0.15 ± 0.003
Xlu5P, reductive	K_m^{Xlu5P}	0.65 ± 0.03	K_m^{NADPH}	0.24 ± 0.01	$K_m^{Xlu5P,\ NADPH}$	0.86 ± 0.04	$V_{max}^{Xlu5P,\ NADPH}$	1.2 ± 0.02
Arb1P, oxidative	K_m^{Arb1P}	3.6 ± 0.2	$K_m^{NADP^+}$	2.7 ± 0.1	$K_m^{Arb1P,\ NADP^+}$	12.8 ± 0.6	$V_{max}^{Arb1P,\ NADP^+}$	0.09 ± 0.002

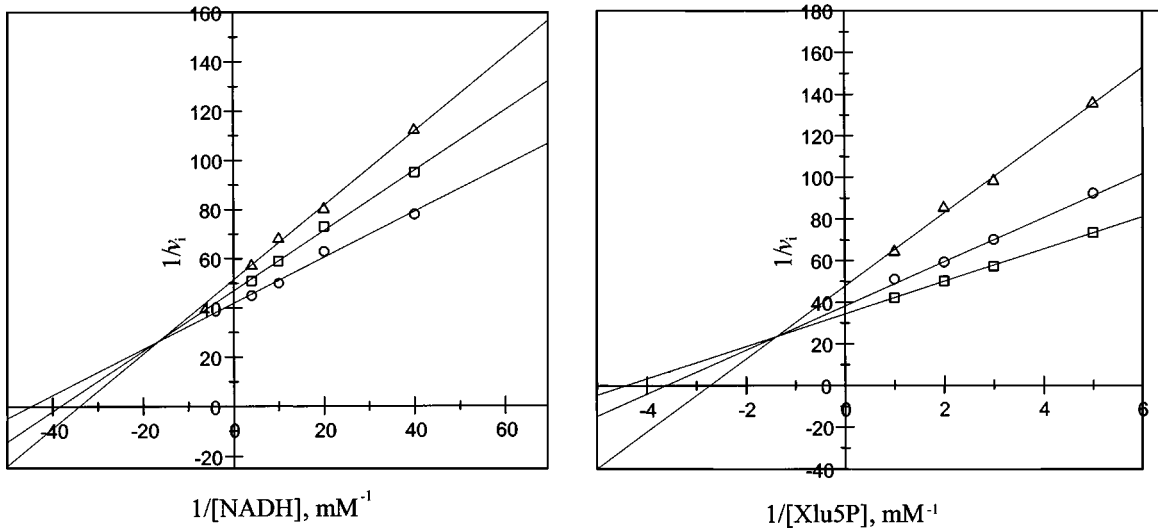

Figure 2 Initial velocities of APDH-catalysed reactions with Xlu5P as the substrate

Left-hand panel: fixed Xlu5P concentrations were 0.75 mM (○), 0.5 mM (□) and 0.35 mM (△). Right-hand panel: fixed NADH concentrations were 0.25 mM (□), 0.1 mM (○) and 0.05 mM (△).

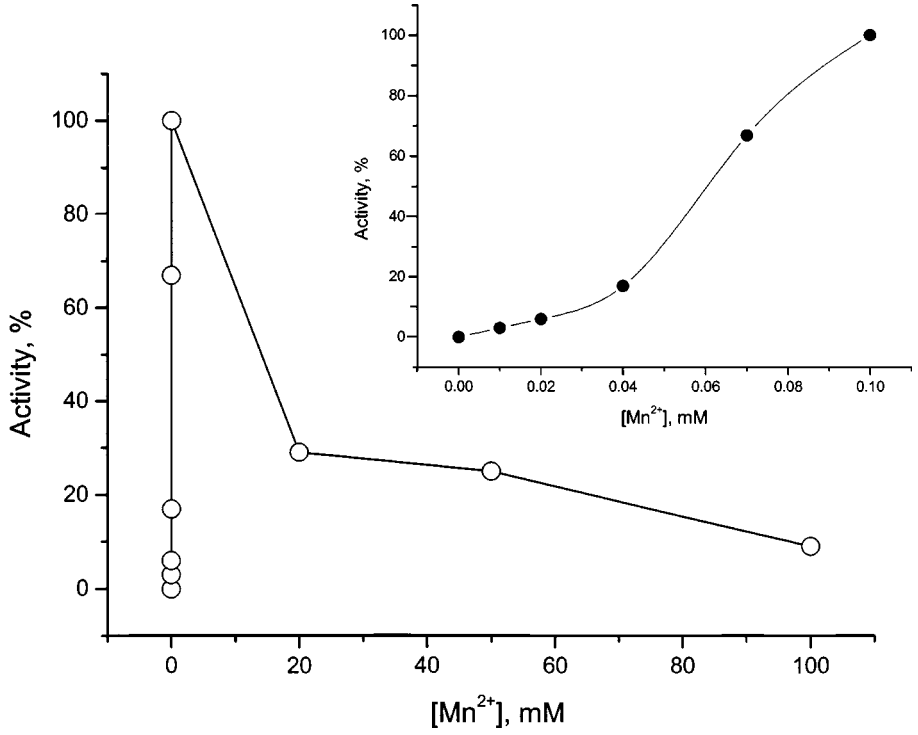

Figure 3 Effect of Mn^{2+} concentration on EDTA-inactivated APDH

Insert: reconstitution of EDTA-inhibited APDH at lower Mn^{2+} concentrations (0–100 μM). Apo-APDH obtained as described in the Materials and methods section was diluted 100-fold (to 0.02 mg/ml, 0.12 μM) in 20 mM Tris/HCl, pH 7.2. $MnCl_2$ was added to 100 μl aliquots of the diluted apo-enzyme to a final concentration of 10 μM–100 mM. The mixtures were incubated for 30 min at 20 °C, followed by further 10-fold dilution into a solution containing 20 mM Tris/HCl, pH 7.2, 1 mM DTT, 0.07 mM NADH and 0.2 mM Xlu5P, and immediate measurement of activity.

per tetramer. Essentially identical results were obtained using the recombinant enzyme purified from *B. subtilis*. Recombinant APDH was also used in the metal ion reconstitution experiments described below. The purified APDH was found to be inactivated by EDTA in a time- and concentration-dependent manner. The second-order rate constant for EDTA inactivation at 20 °C measured as described in the Materials and methods section was 12.2 $M^{-1} \cdot s^{-1}$. Inactive EDTA-modified enzyme contained less than 0.1 mol of Mn^{2+} per tetramer. Analytical gel filtration on a Superose 12 column in the presence of 1 mM EDTA and native

MSKTMKGVSKQAPGYDQMAFIDLSVPEATDDKVLIKVAYTGICGSDIHTF

KGEYK**NPTTPVVLGHEF**SGQVVEVGANVTKVKVGDRVTSETTFYVCGECD

YCKEK**QYNLCPHR**KGIGTQQNGSMANYVLAREESIHLLPDHLSYEGAAMS

EPLACCVHAMYQKSHLELKDTIIIMGPGPIGLYLLQIAKEIGAFVIMTGI

TKDAHRLALAK**KLGADVIVDTMK**EDLAK**VVNEITDGYGVDK**VYDASGAVP

AVNASLPLIR**KQGQFIQVGLFANK**MVDLDTESIIQR**EIEYIGSR**SQNPYD

WPIAIHLLAK**GAINIDEMITK**KYPLTEWREAFDKVMEGNEIKVMIESNPE

EF

Figure 4 Deduced amino acid sequence of the APDH from *E. avium*

The underlined sequences correspond to peptides detected in the MALDI-TOF (matrix-assisted laser-desorption ionization–time-of-flight) mass map of the in-gel-digested native APDH. The sequences shown in bold were determined by purification and Edman sequence analysis.

gel electrophoresis showed that APDH treated with EDTA retained its tetrameric structure. Xlu5P did not protect the enzyme from EDTA inactivation. The EDTA-inactivated APDH was treated with several bivalent cations (Ca^{2+}, Mg^{2+}, Zn^{2+}, Mn^{2+} and Fe^{2+}) in a concentration range of 0.1–20 mM. Only the addition of Mn^{2+} at concentrations of up to 2 mM resulted in complete re-activation of APDH. The specific activity of the re-activated enzyme was 12 ± 1 units/mg, similar to the non-treated APDH. The pH optimum for the Mn^{2+}-dependent restoration of the enzyme was studied by steady-state kinetics using Xlu5P as a substrate and was about 7.0 ± 0.5. The enzyme restored after Mn^{2+} treatment also contained 4.05 ± 0.05 ions/tetramer. Mn^{2+} ions at concentrations above 10 mM inhibited APDH activity (Figure 3). Similarly to the yeast Mn^{2+}-dependent enolase [27], this may be explained by the presence of an additional Mn^{2+}-binding site in the enzyme molecule. Indeed, increasing the concentration of Mn^{2+} up to 20 mM led to incorporation of 6.05 ions/tetramer, and up to 30 mM resulted in 8.0 ± 1 ions/tetramer. PHMB, Hg^{2+} and Zn^{2+} ions at a concentration of 2 mM completely inactivated APDH. It is well known that in most medium-chain dehydrogenases Zn^{2+} plays the role of metal cofactor, although in some enzymes, for example bovine lens sorbitol dehydrogenase, either Zn^{2+} or Mn^{2+} can function interchangeably [28]. In APDH, Mn^{2+} appears to be the only acceptable cofactor ion. Thus, the metal-ion dependency of APDH is different from that of threonine dehydrogenase, where both Zn^{2+} and Mn^{2+} are required for maximum activity [29].

Peptide sequences that were determined from the purified APDH are shown in Figure 4. Using degenerate oligonucleotides derived from five of these sequences (Pep1, QYNLCPHR; Pep2, EIEYIGSR; Pep3, KQGQFIQVGLFANK; Pep4, GAINIDEMITK; Pep5, VVNEITDGYGVDK) numerous PCR products were generated. The largest product (about 650 bp) was obtained with the primer pair oXP-1F (5′-CARTATAATTTNTGTCCNGTTMG-3′) and oXP-4R (5′-ATCATTTCRTCNATRTTNATNGCNC-3′), corresponding to Pep1 and Pep4, respectively. This product was cloned and used to screen the *E. avium* genomic library. One hybridization-positive clone containing the smallest insert was sequenced (the sequence has been deposited with GenBank under accession number AY078980). The deduced functional map of the sequenced DNA fragment is shown in Figure 5. Four open reading frames can be identified within it (the start of frame 1 is outside of the sequenced area). The amino acid sequences of the products of these open reading frames were compared with the GenBank database using the BLASTP service of NCBI. Open reading frames (Orfs) 1 and 3 show high homology to components of the galactitol-PTS of *Escherichia coli* and *Salmonella typhimurium*. The highest-scoring homologue of Orf2 is a component of the PTS system in *Listeria monocytogenes*. The sequence of Orf4 encodes the APDH. All the sequenced peptides were found within the translated sequence of Orf4 (Figure 4). Homology comparisons of the APDH sequence place it within the large family of medium-chain polyol/alcohol dehydrogenases [18]. The strongest matches are found to the proteins deduced from the genomic DNA sequences of several Gram-positive species, particularly from *L. monocytogenes* (GenBank accession number NP_466185.1), *Listeria inocua* (NP_472141.1), *Staphylococcus aureus* (NP_002758) and *B. halodurans* (NP_002570). None of these proteins has been characterized biochemically. In comparison with these homologues, all the enzymes with known substrate specificity are more distantly related to APDH. Among such enzymes, bacterial sorbitol dehydrogenases (also referred to as polyol or xylitol dehydro-

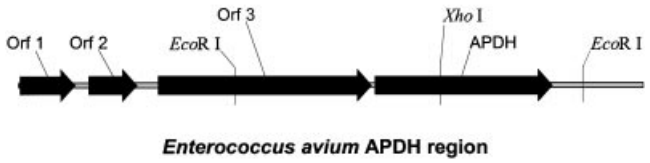

Figure 5 The chromosomal area of *E. avium* around the APDH gene

Orfs 1 and 3 are homologous to components of the galactitol-PTS from *Salmonella typhimurium* and *Escherichia coli*. The closest homologue of Orf2 is a component of the arabitol-PTS system from *Listeria monocytogenes*.

genases) show the closest match. All known sequences of hexitol- and tetritol-phosphate dehydrogenases show much weaker homology, indicating that polyol-phosphate dehydrogenases do not form a common evolutionary branch.

The whole coding sequence of Orf4 was amplified by PCR and placed under control of a *degQ*36M promoter from *B. subtilis* in a plasmid named pGTK74(APDH3). *B. subtilis* transformed with this plasmid expressed APDH at a level of about one-third of the total soluble protein. The enzyme was purified from the cell extract of *B. subtilis* to near homogeneity using Sepharose-Blue chromatography. The kinetic characteristics of the recombinant enzyme were measured in both oxidative and reductive reactions. The results were essentially identical with those obtained with the enzyme isolated from *E. avium*.

In order to verify that high-scoring homologues of APDH identified in genomic sequences share the substrate specificity with the enzyme from *E. avium*, we have amplified and expressed an open reading frame from the genomic sequence of *B. halodurans*. Indeed, the recombinant enzyme from *B. halodurans* was found to catalyse the reduction by NADH of both Xlu5P and Rlu5P, but not any of the neutral keto-sugars. Arabitol was the only polyol found among the dephosphorylated reaction products of Xlu5P and Rlu5P. This result strongly suggests that other uncharacterized genomic open reading frames with even higher homology than that of the *B. halodurans* enzyme (in the genomes of *L. monocytogenes*, *L. inocua* and *S. aureus*) also encode APDH. Moreover, when we fractionated protein extracts of *L. casei* strain CL-83 8 [5] induced by growth on xylitol, both xylitol-phosphate dehydrogenase and APDH were isolated (results not shown). In the case of *Listeria*, the conclusion that this bacterium assimilates arabitol via the arabitol phosphate route is supported by the findings of Saklani-Justoforges et al. [30]. These authors have mapped a mutation that leads to the inability of *L. monocytogenes* to assimilate arabitol to a component of the PTS system. The APDH gene homologue identified in our searches is located in the same apparent operon. Taken together, these findings provide strong evidence that assimilation of arabitol via the arabitol phosphate route is fairly widespread among taxonomically distant Gram-positive species of bacteria.

The strong preference of APDH for Arb1P argues in favour of a hypothesis that D-arabitol is assimilated in *E. avium* via route 3 of Scheme 1. However, theoretically, it may also be possible that both routes 3 and 4 in Scheme 1 operate in parallel. Biochemical studies of the arabitol-PTS in *E. avium* would be needed to resolve this question.

We thank Maija Karhunen for her excellent technical assistance and Janne Kerovuo for re-sequencing the APDH gene. We gratefully acknowledge the contributions of Håkan Gros, Andrew Morgan and Heikki Ojamo to this work through stimulating discussions and encouragement. Vijay Kumar kindly read and commented on the manuscript. Thanks are due to Jack London (National Institute of Dental Research, Bethesda, MD, U.S.A.) for providing us with *L. casei* strain CL83.

REFERENCES

1 Wehmeier, U. F. and Lengeler, J. W. (1994) Sequence of the *sor*-operon for L-sorbose utilization from *Klebsiella pneumoniae* KAY2026. Biochim. Biophys. Acta **1208**, 348–351
2 Novotny, M. J., Reizer, J., Esch, F. and Saier, Jr, M. H. (1984) Purification and properties of D-mannitol-1-phosphate dehydrogenase and D-glucitol-6-phosphate dehydrogenase from *Escherichia coli*. J. Bacteriol. **159**, 986–990
3 Honeyman, A. L. and Curtiss, 3rd, R. (1992) Isolation, characterization, and nucleotide sequence of the *Streptococcus mutans* mannitol-phosphate dehydrogenase gene and the mannitol-specific factor III gene of the phosphoenolpyruvate phosphotransferase system. Infect. Immun. **60**, 3369–3375
4 Nobelmann, B. and Lengeler, J. W. (1995) Sequence of the *gat* operon for galactitol utilization from a wild-type strain EC3132 of *Escherichia coli*. Biochim. Biophys. Acta **1262**, 69–72
5 London, J. and Chace, N. M. (1977) New pathways for the metabolism of pentitols. Proc. Natl. Acad. Sci. U.S.A. **74**, 4296–4300
6 Hausman, S. Z. and London, J. (1987) Purification and characterization of ribitol-5-phosphate and xylitol-5-phosphate dehydrogenases from strains of *Lactobacillus casei*. J. Bacteriol. **169**, 1651–1655
7 Waler, S. M., Rolla, G., Assev, S. and Ciardi, J. E. (1984) The effect of xylitol on plaque metabolism. Swed. Dent. J. **8**, 155–161
8 Scangos, G. A. and Reiner, A. M. (1978) Ribitol and D-arabitol catabolism in *Escherichia coli*. J. Bacteriol. **134**, 492–500
9 Neuberger, M. S., Patterson, A. R. A. and Hartley, B. S. (1979) Purification and properties of *Klebsiella aerogenes* arabitol dehydrogenase. Biochem. J. **183**, 31–42
10 Wong, B., Leeson, S., Grindle, S., Magee, B., Brooks, E. and Magee, P. T. (1995) D-Arabitol metabolism in *Candida albicans*: construction and analysis of mutants lacking D-arabitol dehydrogenase. J. Bacteriol. **177**, 2971–2976
11 Barnwell, J. L., Saunders, W. A. and Watson, R. W. (1955) Synthesis and characterization of D-xylofuranose-5-phosphate. Can. J. Chem. **33**, 711–715
12 Savel'ev, A. N., Eneyskaya, E. V., Isaeva-Ivanova, L. S., Shabalin, K. A., Golubev, A. M. and Neustroev, K. N. (1997) The carbohydrate moiety of α-galactosidase from *Trichoderma reesei*. Glycoconj. J. **14**, 897–905
13 Laemmli, U. K. (1970) Cleavage of structural proteins during the assembly of the head of bacteriophage T4. Nature (London) **227**, 680–685
14 Lowry, O. H., Rosenbrough, N. J., Farr, A. L. and Randall, R. J. (1951) Protein measurements with the Folin phenol reagent. J. Biol. Chem. **193**, 265–275
15 Sambrook, J., Fritsch, E. F. and Maniatis, T. (1989) Molecular Cloning: a Laboratory Manual, 2nd edn, Cold Spring Harbor Press, Cold Spring Harbor, NY
16 Omburo, G. A., Kuo, J. M., Mullins, L. S. and Raushel, F. M. (1992) Characterization of the zinc binding site of bacterial phosphotriesterase. J. Biol. Chem. **267**, 13278–13283
17 Kayestha, R. Sumati and Hajela, K. (1995) ESR studies on the effect of ionic radii on displacement of Mn^{2+} bound to a soluble β-galactoside binding hepatic lectin. FEBS Lett. **368**, 285–288
18 Heppel, S., Harkness, D. and Hilmoe, R. (1962) A study of the substrate specificity and other properties of the alkaline phosphatase of *Escherichia coli*. J. Biol. Chem. **237**, 841–845
19 Jörnvall, H., Danielson, O., Ecklund, H., Helmqvist, L., Höög, J.-O., Pares, X. and Shafcat, J. (1993) Enzyme and isoenzyme developments within the medium-chain alcohol dehydrogenase family. In Enzymology and Molecular Biology of Carbonyl Metabolism, vol. 4 (Weiner, H., Crabb, D. and Flynn, T. G., eds.), pp. 533–544, Plenum, New York
20 Nyman, T. A., Matikainen, S., Sareneva, T., Julkunen, I. and Kalkkinen, N. (2000) Proteome analysis reveals ubiquitin-conjugating enzymes to be a new family of interferon-α-regulated genes. Eur. J. Biochem. **267**, 4011–4019
21 Dorokhov, Y. L., Mäkinen, K., Frolova, O. Y., Merits, A., Saarinen, J., Kalkkinen, N., Atabekov, J. G. and Saarma, M. (1999) A novel function for a ubiquitous plant enzyme pectin methylesterase: the host-cell receptor for the tobacco mosaic virus movement protein. FEBS Lett. **461**, 223–228
22 Cutting, S. M. and Vander Horn, P. B. (1990) Genetic analysis. In Molecular Biological Methods for *Bacillus* (Harwood, C. R. and Cutting, S. M., eds.), pp. 27–74, John Wiley and Sons, Chichester
23 Kerovuo, J., von Weymarn, N., Povelainen, M., Auer, S. and Miasnikov, A. (2000) A new efficient expression system for *Bacillus* and its application to production of recombinant phytase. Biotechnol. Lett. **22**, 1311–1317
24 Yang, M., Ferrari, E., Chen, E. and Henner, D. J. (1986) Identification of the pleiotropic *sacQ* gene of *Bacillus subtilis*. J. Bacteriol. **166**, 113–119
25 Hueck, C. J., Hillen, W. and Saier, M. H. (1994) Analysis of a sequence mediating catabolite repression in Gram-positive bacteria. Res. Microbiol. **145**, 503–518
26 Bron, S. (1990) Plasmids. In Molecular Biological Methods for *Bacillus* (Harwood, C. R. and Cutting, S. M., eds.), pp. 148–149, John Wiley and Sons, Chichester
27 Lee, B. H. and Nowak, T. (1992) Influence of pH on the Mn^{2+} activation of and binding to yeast enolase: functional study. Biochemistry **31**, 2165–2171
28 Marini, I., Bucchioni, L., Borella, P., Del Corso, A. and Mura, U. (1997) Sorbitol dehydrogenase from bovine lens: purification and properties. Arch. Biochem. Biophys. **340**, 383–391
29 Epperly, B. R. and Dekker, E. E. (1991) L-Threonine dehydrogenase from *Escherichia coli*. Identification of an active site cysteine residue and metal ion studies. J. Biol. Chem. **266**, 6086–6092
30 Saklani-Justoforges, H., Fontan, E. and Goosens, P. L. (2001) Characterisation of a *Listeria monocytogenes* mutant deficient in D-arabitol fermentation. Res. Microbiol. **152**, 175–177

Received 11 July 2002/20 November 2002; accepted 6 December 2002
Published as BJ Immediate Publication 6 December 2002, DOI 10.1042/BJ20021096